MATHEMATICAL BIOSCIENCES
AND ENGINEERING
Volume **3**, Number **3**, July **2006**

http://www.mbejournal.org/

pp. **445–458**

STOCHASTIC EPIDEMIC MODELS WITH A BACKWARD BIFURCATION

Linda J. S. Allen

Department of Mathematics and Statistics
Texas Tech University, Lubbock, TX 79409-1042

P. van den Driessche

Department of Mathematics and Statistics
University of Victoria, Victoria, BC V8W 3P4, Canada

Abstract. Two new stochastic epidemic models, a continuous-time Markov chain model and a stochastic differential equation model, are formulated. These are based on a deterministic model that includes vaccination and is applicable to pertussis. For some parameter values, the deterministic model exhibits a backward bifurcation if the vaccine is imperfect. Thus a region of bistability exists in a subset of parameter space. The dynamics of the stochastic epidemic models are investigated in this region of bistability, and compared with those of the deterministic model. In this region the probability distribution associated with the infective population exhibits bimodality with one mode at the disease-free equilibrium and the other at the larger endemic equilibrium. For population sizes $N \geq 1000$, the deterministic and stochastic models agree, but for small population sizes the stochastic models indicate that the backward bifurcation may have little effect on the disease dynamics.

1. **Introduction.** Two stochastic epidemic models are formulated based on an epidemic model applicable to pertussis. The epidemic model includes vaccination and is referred to as an SIVRS epidemic model, where the classes (disease states) contain susceptible, infective, recovered, and vaccinated individuals. The deterministic model was analyzed by Arino et al. [1] and was shown to exhibit a backward bifurcation for some parameter values if the vaccine is imperfect. There exists a region of bistability in a subset of parameter space with a locally stable endemic equilibrium and a locally stable disease-free equilibrium. Outside the region of bistability, either the disease-free equilibrium or a unique endemic equilibrium is globally stable. Backward bifurcation has also been observed in other epidemic models, for example, multigroup models analysed by Hadeler and coauthors [2, 3]. Our goal in this investigation is to compare the dynamics of the deterministic and the stochastic epidemic models in this region of bistability. The stochastic models are a continuous-time Markov chain model and a stochastic differential equation model. The stochastic differential equation model is a new formulation that is derived from the Markov chain model [4, 5].

2000 *Mathematics Subject Classification.* 92D30.

Key words and phrases. epidemic model, vaccination, bistability, continuous-time Markov chain, stochastic differential equations.

Numerous stochastic models based on the well-known SIS and SIR epidemic models have been used to investigate questions regarding the dynamics of an epidemic. For example, the duration of an epidemic, the probability of an outbreak, the probability that the epidemic ends, the final size distribution, and the quasistationary distribution have been investigated using stochastic models (see, e.g., [6, 7, 8, 9, 10, 11, 12, 13, 14, 15] and references therein). The stochastic epidemic models in these studies have been based primarily on continuous-time Markov chain (CTMC) models and none of these studies have investigated the phenomenon of a backward bifurcation. Here, a new formulation based on stochastic differential equations (SDEs) is presented, and the stochastic dynamics in the region of bistability are investigated.

In the next section, the deterministic pertussis model is described. This model is also applicable for other relatively mild diseases for which an imperfect vaccine is available (e.g., some strains of influenza). Then the CTMC model and the SDE model are formulated based on the deterministic model. It is shown for the SDE model that with large population sizes the variance in the random variables for proportions scales on the order of $1/N$, where N is the total population size. Hence, for large population sizes, there is close agreement between the stochastic and deterministic models. In addition, at the disease-free equilibrium, it is shown that the expected values of the random variables agree with the solution to the deterministic model. Through extensive numerical simulations, the dynamics of the CTMC and the SDE models are investigated with the parameter values chosen within or close to the region of bistability. The probability of disease extinction and the probability distribution for the number of infective individuals are computed and compared to the results for the deterministic model.

2. Model formulations.

First, we describe the deterministic epidemic model that was analyzed by Arino et al. [1]. The model consists of four differential equations, one for each of the four disease states: susceptible, infective, recovered, and vaccinated, with the number in each class denoted by $S(t)$, $I(t)$, $R(t)$, and $V(t)$, respectively. Second, we develop two stochastic models based on the deterministic model, a CTMC model and an SDE model. The stochastic variability in these models is due to the variability in the birth, death, and infection processes and does not account for environmental variability.

2.1. Deterministic model.

The system of differential equations for the deterministic model [1] is

$$\begin{aligned}
\frac{dS}{dt} &= d(N-S) - \beta\frac{SI}{N} - \phi S + \theta V + \nu R,\\
\frac{dI}{dt} &= \beta\frac{SI}{N} + \sigma\beta\frac{VI}{N} - (d+\gamma)I,\\
\frac{dR}{dt} &= \gamma I - (d+\nu)R,\\
\frac{dV}{dt} &= \phi S - (d+\theta)V - \sigma\beta\frac{VI}{N},
\end{aligned} \tag{1}$$

where N is the constant total population size; thus $S(t)+I(t)+R(t)+V(t)=N$. Parameter β is the transmission rate, d is the natural death rate (=birth rate), γ is the recovery rate, ν is the rate of loss of immunity, ϕ is the vaccination rate, and θ is the rate of vaccine waning. For pertussis, realistic parameter values for γ, d,

ϕ, and θ are given in [1, Table 1]; see Table 1 below. Parameters β and ν were chosen to heighten the backward bifurcation effect [1]. For the parameter set chosen, vaccine induced immunity wanes on the order of five years (parameter θ), whereas natural immunity (parameter ν) lasts only a month. This latter assumption may be biologically unrealistic. Natural immunity from pertussis infection may last on the order of years. However, our goal in parameter selection was to emphasize the region of bistability.

TABLE 1. Basic parameter values.

Parameter	Value
β	1/(2.5 days)
γ	1/(21 days)
d	1/(75 years)
ν	1/(31 days)
ϕ	1/(20 days)
θ	1/(5 years)

The vaccine is assumed to be useful but imperfect. Thus the vaccine efficacy, denoted by $1-\sigma$, lies in the interval $(0, 1)$. When $\sigma = 1$, the vaccine is totally useless and when $\sigma = 0$ the vaccine is perfect (vaccination is 100% effective). A similar model that includes input (immigration) of infectives is considered by Alexander et al. [16].

Because the total population size is constant, the number of susceptible individuals can be expressed in terms of the other variables, $S(t) = N - I(t) - R(t) - V(t)$. In addition, the three state variables, I, R, and V, can be expressed as proportions $i = I/N$, $r = R/N$, $v = V/N$, and $s = 1 - i - r - v$. Then model (1) can be simplified as follows:

$$\begin{aligned} \frac{di}{dt} &= \beta si + \sigma\beta vi - (d+\gamma)i \\ \frac{dr}{dt} &= \gamma i - (d+\nu)r \\ \frac{dv}{dt} &= \phi s - (d+\theta)v - \sigma\beta vi. \end{aligned} \tag{2}$$

For some parameter values with $0 < \sigma < 1$, model (1) exhibits a backward bifurcation, which is a result of the vaccine being imperfect [1]. The vaccination reproduction number for model (1) is

$$\mathbf{R}_{vac} = \mathbf{R}_0 \frac{d+\theta+\sigma\phi}{d+\theta+\phi},$$

where $\mathbf{R}_0 = \beta/(d+\gamma)$, the well-known basic reproduction number for an SIR epidemic model without vaccination. If $\sigma = 1$, then $\mathbf{R}_{vac} = \mathbf{R}_0$, and for $0 \le \sigma < 1$, $\mathbf{R}_{vac} < \mathbf{R}_0$. For $\sigma \in [0.08866, 0.10884]$ and the parameter values in Table 1, model (1) exhibits bistability. The bifurcation diagram is illustrated in Figure 1 for the parameter values in Table 1 and $N = 200$. For other population sizes N, the bifurcation diagram has exactly the same shape; the only change is the range on the vertical axis which is approximately $[0, N/4]$ (e.g., for $N = 1000$, the range on the vertical axis is approximately $[0, 250]$). The basic reproduction number $\mathbf{R}_0 = 8.3936 > 1$, but the vaccination reproduction number satisfies $\mathbf{R}_{vac} < 1$ for

$\sigma < 0.10884$ and $\mathbf{R}_{vac} > 1$ for $\sigma > 0.10884$. The region of bistability extends from the saddle node bifurcation at $\sigma = 0.08866$ (corresponding to $\mathbf{R}_{vac} = 0.8326$) to the transcritial bifurcation at $\sigma = 0.10884$ (corresponding to $\mathbf{R}_{vac} = 1$).

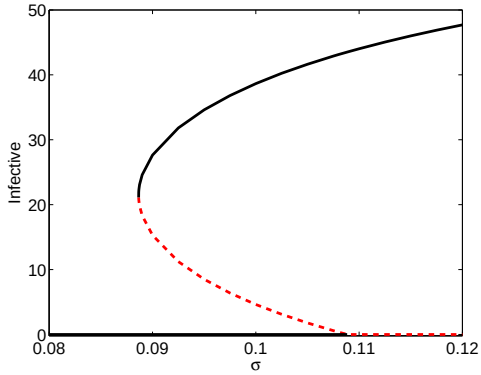

FIGURE 1. Bifurcation diagram for model (1) illustrating the stable (solid curve) and unstable equilibrium values (dashed curve) for the infective state $\bar{I}$ in terms of the bifurcation parameter σ. The basic parameter values are given in Table 1. The total population size is $N = 200$.

2.2. **Continuous-time Markov chain model.** Let $\mathcal{S}(t)$, $\mathcal{I}(t)$, $\mathcal{R}(t)$, and $\mathcal{V}(t)$ denote discrete random variables for the susceptible, infective, recovered, and vaccinated individuals, respectively, at time t. (Random variables are denoted with calligraphic letters.) Because the random variable $\mathcal{S}(t)$ can be expressed in terms of the other random variables, $\mathcal{S}(t) = N - \mathcal{I}(t) - \mathcal{R}(t) - \mathcal{V}(t)$, the CTMC model is described in terms of the dynamics of the three random variables $\mathcal{I}(t)$, $\mathcal{R}(t)$, and $\mathcal{V}(t)$. Then

$$\mathcal{I}(t),\ \mathcal{R}(t),\ \mathcal{V}(t) \in \{0, 1, 2, \ldots, N\}$$

and $\mathcal{I}(t) + \mathcal{R}(t) + \mathcal{V}(t) \leq N$. Let the change in these random variables during the period t to $t + \Delta t$ be denoted as $\Delta\mathcal{I}$, $\Delta\mathcal{R}$ and $\Delta\mathcal{V}$; e.g., $\Delta\mathcal{I} = \mathcal{I}(t + \Delta t) - \mathcal{I}(t)$.

The infinitesimal transition probabilities that describe this multivariate Markov process are given by

$$\begin{aligned}
&\text{Prob}\{(\Delta\mathcal{I}, \Delta\mathcal{R}, \Delta\mathcal{V}) = (i, j, k) | (\mathcal{I}, \mathcal{R}, \mathcal{V})\} \\
&\qquad = \begin{cases}
(\beta\mathcal{S}\mathcal{I}/N)\Delta t + o(\Delta t), & (i, j, k) = (1, 0, 0) \\
d\mathcal{I}\Delta t + o(\Delta t), & (i, j, k) = (-1, 0, 0) \\
\gamma\mathcal{I}\Delta t + o(\Delta t), & (i, j, k) = (-1, 1, 0) \\
(d + \nu)\mathcal{R}\Delta t + o(\Delta t), & (i, j, k) = (0, -1, 0) \\
(\sigma\beta\mathcal{V}\mathcal{I}/N)\Delta t + o(\Delta t), & (i, j, k) = (1, 0, -1) \\
(d + \theta)\mathcal{V}\Delta t + o(\Delta t), & (i, j, k) = (0, 0, -1) \\
\phi\mathcal{S}\Delta t + o(\Delta t), & (i, j, k) = (0, 0, 1),
\end{cases}
\end{aligned} \tag{3}$$

where $\mathcal{I} \equiv \mathcal{I}(t)$, $\mathcal{R} \equiv \mathcal{R}(t)$ and $\mathcal{V} \equiv \mathcal{V}(t)$. The probability of no change,

$$\text{Prob}\{\Delta\mathcal{I}, \Delta\mathcal{R}, \Delta\mathcal{V}) = (0, 0, 0) | (\mathcal{I}, \mathcal{R}, \mathcal{V})\},$$

equals

$$1 - [\beta(\mathcal{S} + \sigma\mathcal{V})\mathcal{I}/N + d(\mathcal{I} + \mathcal{R} + \mathcal{V}) + \gamma\mathcal{I} + \nu\mathcal{R} + \theta\mathcal{V} + \phi\mathcal{S}]\,\Delta t + o(\Delta t).$$

The probabilities of all other changes in state during the time interval Δt are $o(\Delta t)$, and the process is time-homogeneous.

Let lower case letters s, i, r, and v denote the values of the random variables, $\mathcal{S}$, $\mathcal{I}$, $\mathcal{R}$ and $\mathcal{V}$. The joint probability function $p_{irv}(t) = \text{Prob}\{\mathcal{I}(t) = i, \mathcal{R}(t) = r, \mathcal{V}(t) = v\}$ is the solution of the forward Kolmogorov differential equations,

$$\begin{aligned}\frac{dp_{irv}}{dt} &= \beta\frac{(s+1)(i-1)}{N}p_{i-1,r,v} + d(i+1)p_{i+1,r,v} + \gamma(i+1)p_{i+1,r-1,v} \\ &\quad + (d+\nu)(r+1)p_{i,r+1,v} + \sigma\beta\frac{(v+1)(i-1)}{N}p_{i-1,r,v+1} \\ &\quad + \phi(s+1)p_{i,r,v-1} + (d+\theta)(v+1)p_{i,r,v+1} \\ &\quad - [\beta(s+\sigma v)i/N + d(i+r+v) + \gamma i + \nu r + \theta v + \phi s]\,p_{irv}.\end{aligned}$$

For large N, this system of nonlinear differential equations for $i, r, v \in \{0, 1, \ldots, N\}$ and $i + r + v \le N$ becomes very complex.

One alternate method for analyzing the stochastic model behavior is through the expectation and higher moments. Differential equations for the expectation and higher-order moments can be derived for each random variable [17, 18]. However, as in the case for the forward Kolmogorov differential equations, each moment equation depends on higher-order moments that together form an infinite system of differential equations. Isham [17] and Lloyd [18] applied moment closure techniques to SIS, SIR, and SEIR stochastic epidemic models to approximate the higher-order moments in these equations. Their methods reduce the number of differential equations so that approximate solutions can be obtained for the first few moments. There are special cases for which these approximation techniques are not required, since the system simplifies to a linear one.

In the special case $\mathcal{I} \equiv 0$, the joint probability function $p_{rv}(t) = \text{Prob}\{\mathcal{R}(t) = r, \mathcal{V}(t) = v\}$ is linear. Then it easily follows that the differential equations for the expectations of $\mathcal{R}$ and $\mathcal{V}$ do not depend on higher-order moments and are also linear; i.e.,

$$\begin{aligned}\frac{d\mathbf{E}(\mathcal{R}(t))}{dt} &= -(d+\nu)\mathbf{E}(\mathcal{R}(t)), \\ \frac{d\mathbf{E}(\mathcal{V}(t))}{dt} &= \phi\mathbf{E}(\mathcal{S}(t)) - (d+\theta)\mathbf{E}(\mathcal{V}(t)),\end{aligned} \tag{4}$$

where $\mathbf{E}(\mathcal{S}(t)) = N - \mathbf{E}(\mathcal{R}(t)) - \mathbf{E}(\mathcal{V}(t))$. Note that the preceding system of differential equations agrees with (1) when $I(t) \equiv 0$. That is, the solutions for the expectations of the random variables $\mathcal{R}$ and $\mathcal{V}$ in (4) are equal to those for R and V in (1) when $I(t) \equiv 0$ and the initial conditions are equal, namely, $R(0) = \mathbf{E}(\mathcal{R}(0))$ and $V(0) = \mathbf{E}(\mathcal{V}(0))$. Since our goal is to study the behavior when $\mathcal{I} \not\equiv 0$, we use numerical simulations based on the transition probabilities (instead of applying the forward Kolmogorov equations or moment closure techniques) to study the stochastic model behavior.

2.3. **Stochastic differential equation model.** To derive an SDE model, let $\mathcal{I}(t)$, $\mathcal{R}(t)$, and $\mathcal{V}(t)$ denote continuous random variables for the number of infective, recovered, and vaccinated individuals, respectively, at time t. Let $\mathcal{X}(t)$ denote the

random vector, $\mathcal{X}(t) = (\mathcal{I}(t), \mathcal{R}(t), \mathcal{V}(t))^T$. Then

$$\mathcal{I}(t),\ \mathcal{R}(t), \mathcal{V}(t) \in [0, N]$$

and $\mathcal{I}(t) + \mathcal{R}(t) + \mathcal{V}(t) \leq N$. A system of SDEs can be derived by applying the transition probabilities (3) for a fixed time step Δt. The method of derivation is described briefly (for more details see [4, 5]).

Let $\Delta\mathcal{X}(t) = \mathcal{X}(t + \Delta t) - \mathcal{X}(t) = (\Delta\mathcal{I}(t), \Delta\mathcal{R}(t), \Delta\mathcal{V}(t))^T$ denote the random vector for the change in the random variables during the time interval Δt. Assume $\Delta\mathcal{X}(t)$ is normally distributed. The expectation vector $\mathbf{E}(\Delta\mathcal{X}(t))$ and the covariance matrix $\Sigma(\Delta\mathcal{X}(t))$ associated with $\Delta\mathcal{X}(t)$ are now computed. Based on the infinitesimal transition probabilities (3), the expected change to order Δt is

$$\begin{aligned}\mathbf{E}(\Delta\mathcal{X}(t)) &= \begin{pmatrix} \beta\dfrac{\mathcal{S}\mathcal{I}}{N} + \sigma\beta\dfrac{\mathcal{V}\mathcal{I}}{N} - (d+\gamma)\mathcal{I} \\ \gamma\mathcal{I} - (d+\nu)\mathcal{R} \\ \phi\mathcal{S} - (d+\theta)\mathcal{V} - \sigma\beta\dfrac{\mathcal{V}\mathcal{I}}{N} \end{pmatrix}\Delta t + o(\Delta t) \\ &= \mu(\mathcal{X}(t))\Delta t + o(\Delta t),\end{aligned}$$

where $\mathcal{I} \equiv \mathcal{I}(t)$, $\mathcal{R} \equiv \mathcal{R}(t)$, $\mathcal{V} \equiv \mathcal{V}(t)$ and $\mathcal{S} \equiv \mathcal{S}(t) = N - \mathcal{I}(t) - \mathcal{R}(t) - \mathcal{V}(t)$. Notice that the expectation vector has the same form as the system of ordinary differential equations (1).

The covariance matrix to order Δt is a positive definite symmetric matrix of the form

$$\begin{aligned}\Sigma(\Delta\mathcal{X}(t)) &= \begin{pmatrix} c_{11} & c_{12} & c_{13} \\ c_{12} & c_{22} & 0 \\ c_{13} & 0 & c_{33} \end{pmatrix}\Delta t + o(\Delta t) \\ &= C(\mathcal{X}(t))\Delta t + o(\Delta t),\end{aligned}$$

where the entries of the matrix $C(\mathcal{X}(t))$ are

$$\begin{aligned} c_{11} &= \beta\frac{\mathcal{S}\mathcal{I}}{N} + \sigma\beta\frac{\mathcal{V}\mathcal{I}}{N} + (d+\gamma)\mathcal{I}, \\ c_{22} &= \gamma\mathcal{I} + (d+\nu)\mathcal{R}, \\ c_{33} &= \phi\mathcal{S} + (d+\theta)\mathcal{V} + \sigma\beta\frac{\mathcal{V}\mathcal{I}}{N} \\ c_{12} &= -\gamma\mathcal{I} \\ c_{13} &= -\sigma\beta\frac{\mathcal{V}\mathcal{I}}{N}. \end{aligned}$$

By assumption for small Δt,

$$\Delta\mathcal{X}(t) \sim \mathbf{N}(\mu(\mathcal{X}(t))\Delta t, C(\mathcal{X}(t))\Delta t).$$

Because $C(\mathcal{X}(t))$ is positive definite, it has a unique square root denoted as $A(\mathcal{X}(t)) = \sqrt{C(\mathcal{X}(t))}$ [19]. The random vector $\Delta\mathcal{X}(t)$ can be expressed in a simpler form using the standard normal vector $\eta = (\eta_1, \eta_2, \eta_3)^T \sim \mathbf{N}(0, \mathbf{I})$, where $\mathbf{I}$ is the 3×3 identity matrix,

$$\Delta\mathcal{X}(t) \approx \mu(\mathcal{X}(t))\Delta t + A(\mathcal{X}(t))\sqrt{\Delta t}\,\eta.$$

Therefore,

$$\mathcal{X}(t + \Delta t) = \mathcal{X}(t) + \Delta\mathcal{X}(t) \approx \mathcal{X}(t) + \mu(\mathcal{X}(t))\Delta t + A(\mathcal{X}(t))\sqrt{\Delta t}\,\eta \qquad (5)$$

has an approximate normal distribution,

$$\mathcal{X}(t+\Delta t) \sim \mathbf{N}(\mathcal{X}(t)+\mu(\mathcal{X}(t))\Delta t, C(\mathcal{X}(t))\Delta t).$$

Equation (5) is an Euler approximation of an Itô SDE for $\mathcal{X}(t)$ with time step Δt [20, 21]. If μ and A satisfy certain smoothness and growth conditions in the time and the state variables, then $\mathcal{X}(t)$ converges in the mean square sense as $\Delta t \to 0$ to the solution of the Itô SDE

$$\frac{d\mathcal{X}(t)}{dt} = \mu(\mathcal{X}(t)) + A(\mathcal{X}(t))\frac{d\mathcal{W}(t)}{dt}, \tag{6}$$

where $\mathcal{W}(t) = (\mathcal{W}_1(t), \mathcal{W}_2(t), \mathcal{W}_3(t))^T$ is a 3-dimensional Wiener process [21]. The terms $\mu(\mathcal{X}(t))$ and $A(\mathcal{X}(t))$ are known as the drift and diffusion terms, respectively. If the diffusion term is set to zero, then (6) has the same form as the ordinary differential equations in (1).

The SDEs can be simplified further by considering proportions. Let the random variables for proportions be scaled by the population size (denoted by bold face letters): $\mathbf{i} = \mathcal{I}/N$, $\mathbf{r} = \mathcal{R}/N$, $\mathbf{v} = \mathcal{V}/N$, and $\mathbf{s} = 1 - (\mathbf{i} + \mathbf{r} + \mathbf{v})$, where N is the constant population size. Dividing $\mathcal{X} = (\mathcal{I}, \mathcal{R}, \mathcal{V})^T$ given in (6) by N leads to

$$\frac{d(\mathcal{X}(t)/N)}{dt} = \frac{\mu(\mathcal{X}(t))}{N} + \frac{A(\mathcal{X}(t))}{N}\frac{d\mathcal{W}(t)}{dt}, \tag{7}$$

where

$$\frac{A(\mathcal{X}(t))}{N} = \frac{\sqrt{C(\mathcal{X}(t))/N}}{\sqrt{N}} = \frac{\sqrt{\tilde{C}(\mathcal{X}(t))}}{\sqrt{N}}.$$

Matrix $C(\mathcal{X}(t))/N = \tilde{C}(\mathcal{X}(t)) = (\tilde{c}_{ij})$ is a symmetric matrix with entries $\tilde{c}_{ij}$ the same as c_{ij}, except S, I, R, V, and N are replaced by s, i, r, v, and 1, respectively. In this case, the diffusion term is proportional to $1/\sqrt{N}$, as in Kurtz [22], and the variance for the change in proportions is proportional to $1/N$. When $\mathbf{i} = 0$ the expectations of the random variables $\mathbf{r}$ and $\mathbf{v}$ satisfy the same system of differential equations as the deterministic model in (2).

Kurtz [22] was the first to state that for sufficiently large population sizes N solutions to the CTMC and the SDE models are close but he did not provide a derivation for this relationship. In our derivation, convergence from the Markov chain model to the SDE model depends on the discrete time step $\Delta t \to 0$ and the assumption of normality on the change of the population size. Our derivation provides a straightforward method for formulating the SDE model based on the CTMC model. In addition, our formulation of the SDE model in (7) shows that the variance for the change in proportions $d(\mathcal{X}/N)/dt$ is inversely proportional to the population size. These relationships among the ODE and the stochastic models are very useful but are not well known in mathematical epidemiology.

3. **Numerical examples.** Stochastic epidemic models often have expected values that are close to the solution of their analogous deterministic model when a unique endemic equilibrium exists, provided the population size N and the initial conditions are not too small. For small population sizes or small initial conditions, the stochastic effects may cause population or disease extinction. In the case of bistability, other factors may be significant, such as the size of the basin of attraction for the equilibria. Stochastic sample paths may enter different basins of attraction and tend toward either equilibrium [23, 24].

In the next two subsections, the probability that the epidemic ends (probability of disease extinction) and the probability distribution associated with the infective population are investigated for different population sizes and initial conditions. First, the probability of disease extinction is numerically approximated in the CTMC model for a range of population sizes. Then the probability distribution (quasistationary distribution) associated with the random variable $\mathcal{I}(t)$ is approximated for large N after a period of five years for parameter values within the region of bistability. The CTMC model is used for most of the numerical computations. The SDE model is used to compute the probability distribution for infectives for large N and is compared to the distribution of the CTMC model.

3.1. **Probability of disease extinction.** Three different population sizes, $N = 50$, 200, and 1000, are considered. For $\sigma = 0.08$, 0.10, and 0.12, the probability that the epidemic ends (disease extinction) is computed as a function of time; that is,

$$\text{Prob}\{\mathcal{I}(t) = 0\}$$

for t over a five-year period. When the epidemic ends, the stochastic model approaches the disease-free equilibrium (an absorbing state). This asymptotic behavior always occurs in the stochastic model but the time until absorption can be extremely long, especially for large population sizes. Therefore, we compare the dynamics of the deterministic and the stochastic models for a period of time up to five years. The asymptotic dynamics for the deterministic model at the three values of σ are quite different from the stochastic model. For the deterministic model, at $\sigma = 0.08$, the disease-free equilibrium is globally stable. At $\sigma = 0.10$, there are two endemic equilibria and the disease-free equilibrium, the endemic equilibrium with the larger number of infectives is locally stable as well as the disease-free equilibrium (region of bistability). At $\sigma = 0.12$, there is a globally stable endemic equilibrium (the disease-free equilibrium is unstable). The endemic equilibrium values for the infective state $\bar{I}$ in the deteministic model are given in Table 2.

TABLE 2. Stable (unstable) endemic equilibrium values for the infective state $\bar{I}$.

	σ		
N	0.08	0.10	0.12
50	0	9.662 (1.1556)	11.925
200	0	38.65 (4.622)	47.70
1000	0	193.25 (23.11)	238.5

Based on 5000 sample paths, estimates for the probability of disease extinction are graphed in Figure 2. For $N = 200$ and 1000, the curves for large σ are almost coincident with the time axes. For some values of σ, the probability that the epidemic ends depends on the choice of the initial conditions. Here we chose initial values ($I(0) = 5$, $R(0) = 0$, and $V(0) = 0$) so that the deterministic solution for $\sigma > 0.08866$ approaches the stable endemic equilibrium. For $I(0) = 5$, the infective population size does not immediately hit zero (extinction with probability one). This can be seen in the slight lags in Figure 2, prior to the increase in the probabilities of disease extinction. For $N = 50$, the rapid rise in the probabilities for all three values of σ also illustrates the large impact that stochastic variability

has on small infective population sizes (rapid absorption). After five years (1825 days) the probability of disease extinction for $N = 50$ is greater than 0.79 for all values of σ. This is not the case for $N = 200$ or 1000. The probability of disease extinction when $\sigma = 0.12$ and $N = 200$ is < 0.001 and is even smaller when $\sigma = 0.10$ or 0.12 and $N = 1000$. These results reflect that there is good agreement between the deterministic model and CTMC model for large N.

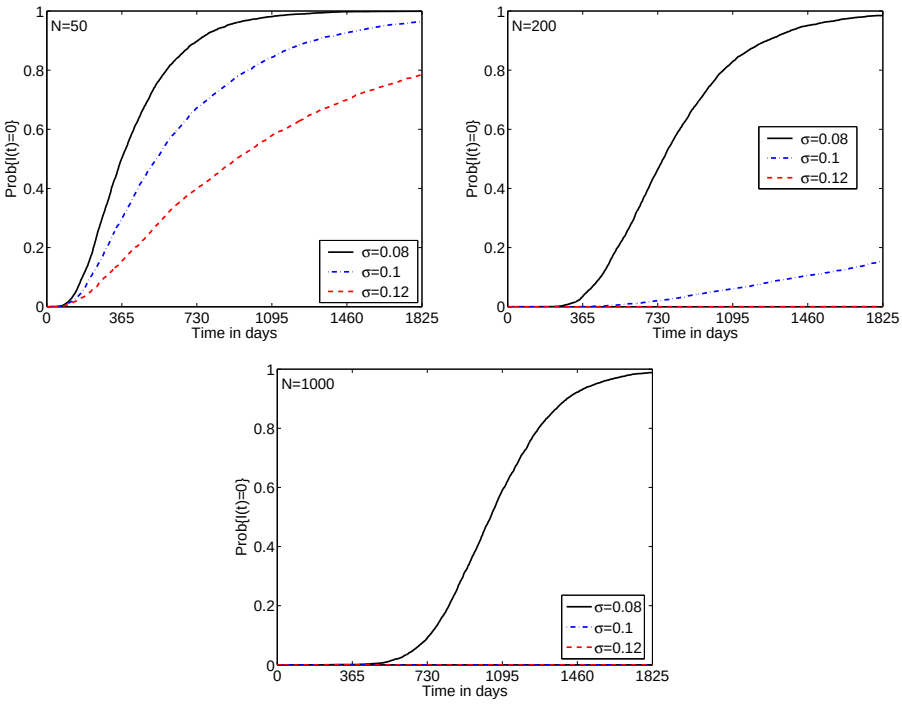

FIGURE 2. Probability of disease extinction for $\sigma = 0.08$, 0.10 and 0.12 with population sizes $N = 50, 200$ and 1000, and initial values for the random variables $\text{Prob}\{\mathcal{I}(0) = 5\} = 1$, $\text{Prob}\{\mathcal{R}(0) = 0\} = 1$, and $\text{Prob}\{\mathcal{V}(0) = 0\} = 1$.

In Figure 3, the probability of disease extinction is compared for $\sigma \in [0.08, 0.12]$ and $N = 50,\ 200$, and 1000 after a period of five years for the same initial conditions as in Figure 2. For $\sigma = 0.08$, the disease is eventually eliminated from the population (with probability one after five years). For the given initial conditions and parameter values, as expected the stochastic and deterministic results are in much better agreement for $N = 1000$ than for the other population sizes. Therefore, to compare the dynamics of the stochastic and the deterministic models in the region of bistability, a population size of $N = 1000$ is used.

3.2. **Probability distribution for the infective population.** The probability distributions associated with the infective population are investigated when parameter values lie within the region of bistability. The parameter values are given in Table 1 for $\sigma \in \{0.09, 0.095, 0.10, 0.105\} \subset [0.08866, 0.10884]$ and $N = 1000$. The stable and unstable endemic equilibrium values are given in Table 3 for $N = 1000$.

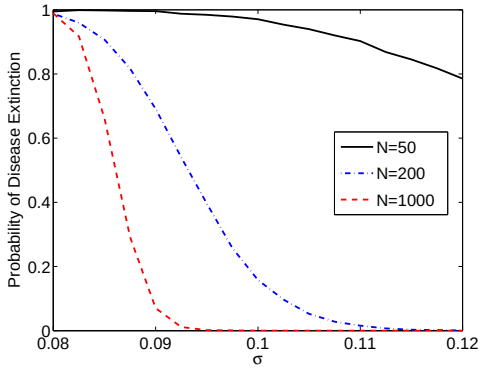

FIGURE 3. Probability of disease extinction after five years for $N = 50$, 200 and 1000 with initial conditions $\text{Prob}\{\mathcal{I}(0) = 5\} = 1$, $\text{Prob}\{\mathcal{R}(0) = 0\} = 1$, and $\text{Prob}\{\mathcal{V}(0) = 0\} = 1$.

The stochastic dynamics in this case depend on the magnitude of σ and the initial conditions. The disease-free equilibrium is $\bar{I} = 0 = \bar{R}$, $\bar{V} = 988.45$, and $\bar{S} = 11.55$. For other population sizes, the equilibrium values are multiples of these values (e.g., for $N = 200 = (1/5)1000$, the equilibrium values are $1/5$ of these values).

TABLE 3. Stable and unstable endemic equilibrium values for the infective, recovered, and vaccinated states, $\bar{I}$, $\bar{R}$, and $\bar{V}$, when $N = 1000$.

	Stable			Unstable		
σ	$\bar{I}$	$\bar{R}$	$\bar{V}$	$\bar{I}$	$\bar{R}$	$\bar{V}$
0.090	138.23	203.82	592.10	76.51	112.81	759.93
0.095	173.06	255.18	500.13	42.53	62.71	857.04
0.100	193.25	284.95	447.41	23.11	34.02	915.19
0.105	208.18	306.96	408.63	8.88	13.09	959.65

Approximations to the probability distribution for the infective state at five years are estimated based on 10,000 sample paths. The approximate probability distributions, $\text{Prob}\{\mathcal{I}(T) = i\}$, $i = 0, 1, 2, \ldots$, for the number of infective individuals are graphed in Figures 4 and 5 with the two sets of figures differing in their initial values. The initial conditions lie in the basin of attraction for the stable endemic equilibrium for the deterministic model except in one case: $\sigma = 0.09$ and $(I(0), R(0), V(0)) = (5, 0, 500)$.

The two modes of the probability distributions are visible in Figures 5 (b), (c), and (d). The mode near the stable endemic equilibrium corresponds to a quasi-stationary distribution (conditional on nonextinction). Increasing the initial value of $\mathcal{V}(0)$ brings the initial values closer to the disease-free equilibrium and a greater number of the sample paths enter the basin of attraction for the disease-free equilibrium (Figure 5 as compared to Figure 4), especially in the case where $\sigma = 0.09$, Figure 5 (a), where the initial condition is in the basin of attraction for the disease-free equilibrium. The proportion of sample paths at the disease-free equilibrium ($\mathcal{I}(t) = 0$ at $t = 1825$ days) for the distributions in Figure 5 at $\sigma = 0.09, 0.095, 0.10,$

and 0.105 are 0.85, 0.49, 0.20, and 0.07, respectively, as compared to those in Figure 4, where the proportion of sample paths at the disease-free equilibrium are 0.08, 0.002, 0.0002, and 0.0002, respectively. These two cases illustrate differences that might exist between initiation of a new vaccination program after an outbreak (Figure 4, $\mathcal{V}(0) = 0$, where no one has been vaccinated) and continuation of a vaccination program (Figure 5, $\mathcal{V}(0) = 500$, where 50% of the population has already been vaccinated).

The normal distribution provides a good fit to the quasistationary distribution when the value of σ is not close to the saddle node bifurcation (dashed curves in Figure 4 (b), (c), and (d) and Figure 5 (d)). The means and variances associated with the quasistationary distribution are approximated from the simulations and are used to graph the normal approximation. The graphs in Figures 4 and 5 are computed from the CTMC model. Simulation results for the SDE model also show close agreement with the results for the CTMC model for both the probability of extinction and the quasistationary distribution.

Close to the saddle node bifurcation ($\sigma = 0.09$), the stochastic model behaves quite differently from the deterministic model. The proximity of the two endemic equilibria, one stable and one unstable, allows sample paths to leave the basin of attraction of the stable endemic equilibrium and pass near the unstable endemic equilibrium (saddle fly-by) [24]. A local stability analysis of the unstable endemic equilibrium for $\sigma = 0.09$ shows that the linearized system of (1) for I, R, and V has two negative eigenvalues and one positive eigenvalue [1]; it is unstable hyperbolic.

4. **Summary.** Two new stochastic epidemic models are formulated to account for the variability inherent in the birth, death, and infection processes, namely, a CTMC model and an SDE model. The stochastic models are used to investigate the dynamics of an epidemic model with parameters applicable to pertussis when the vaccine is imperfect. For a given range of values for the parameter σ (where $1-\sigma$ is the vaccine efficacy), the deterministic model exhibits bistability. The simulations show for population sizes sufficiently large, $N \geq 1000$, the probability distribution associated with the stochastic epidemic models exhibits bimodality as expected in the region of bistability (one mode at the disease-free equilibrium and the other at the endemic equilibrium). For population sizes $N \ll 1000$, the deterministic and the stochastic models differ significantly and a stochastic model provides a more realistic representation of the dynamics. Either the CTMC model or the SDE model can be applied unless population sizes and initial number of infected individuals are very small, $N < 100$, $I(0) \in \{1, 2, 3\}$. In this latter case, the CTMC model is preferred over the SDE model because the CTMC model preserves the discrete population values. These results regarding population size and choice of deterministic versus stochastic model apply to the pertussis model but may hold for more general epidemic models when the population is homogeneously mixed. The particular population size for which one model is selected over another, such as $N = 100$ versus $N = 1000$, will depend on the magnitude of the model parameters in relation to N (see equation (7)). It should be noted, however, that even for large population sizes the deterministic model will not capture the probability of disease extinction when the initial number of infected individuals is small, such as $I(0) \in \{1, 2, 3\}$. In this case, a stochastic model should be applied.

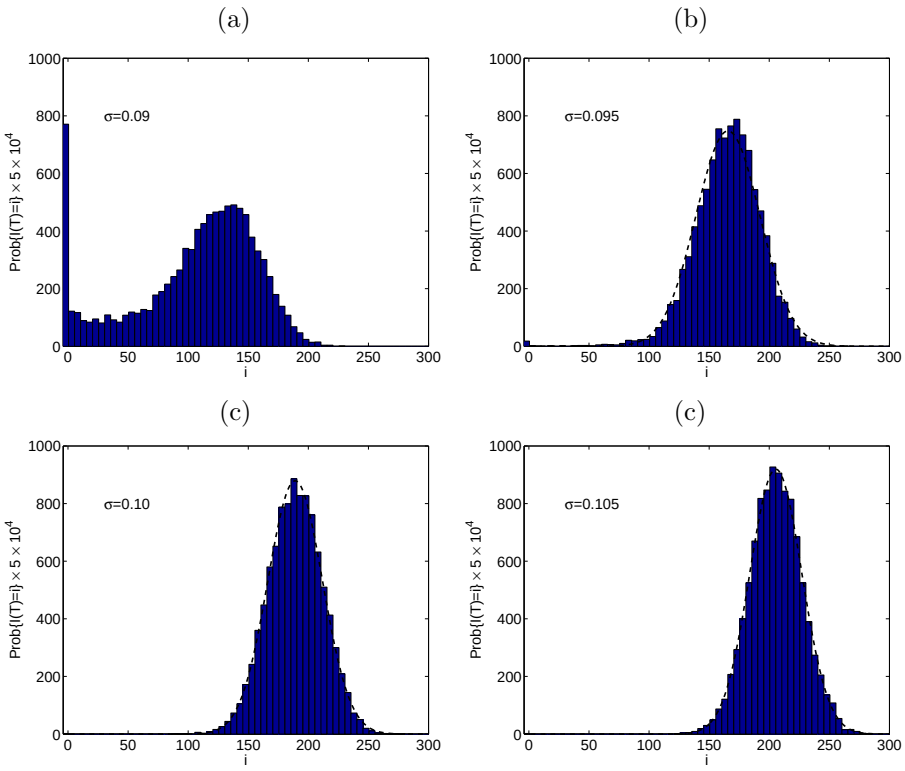

FIGURE 4. Probability distributions at five years for the number of infective individuals given $N = 1000$, $\text{Prob}\{\mathcal{I}(0) = 5\} = 1$, $\text{Prob}\{\mathcal{R}(0) = 0\} = 1$, and $\text{Prob}\{\mathcal{V}(0) = 0\} = 1$. (a) $\sigma = 0.09$, (b) $\sigma = 0.095$, (c) $\sigma = 0.10$, (d) $\sigma = 0.105$. The dashed curves in (b), (c), and (d) are the normal approximations.

The existence of a backward bifurcation in an epidemic model has important public health implications. With a backward bifurcation, it is not sufficient to reduce the vaccination reproduction number to a level below one to eliminate the disease. The vaccination level must be much greater than expected to eliminate the disease (thereby reducing the vaccination reproduction number). However, as shown in the stochastic simulations, this result depends on the population size and the initial values. Based on the parameter values in Table 1, simulations of the CTMC model show for a population size $N = 50$ that there is a high probability of disease extinction for a range of values of the vaccination reproduction number (in this case a stochastic model is required). For a larger population size, $N = 200$, the backward bifurcation is more evident, but it appears that the value of the vaccination reproduction number in relation to one is more important than the effect of the backward bifurcation. Finally for a population size of $N = 1000$, the backward bifurcation is very significant. The simulations for the CTMC model (Figures 4 and 5) indicate that the backward bifurcation may be more important when a new vaccination program is initiated ($\mathcal{V}(0) = 0$) than when a vaccination program has already been in place ($\mathcal{V}(0) = 500$). Thus, depending on the initial values and

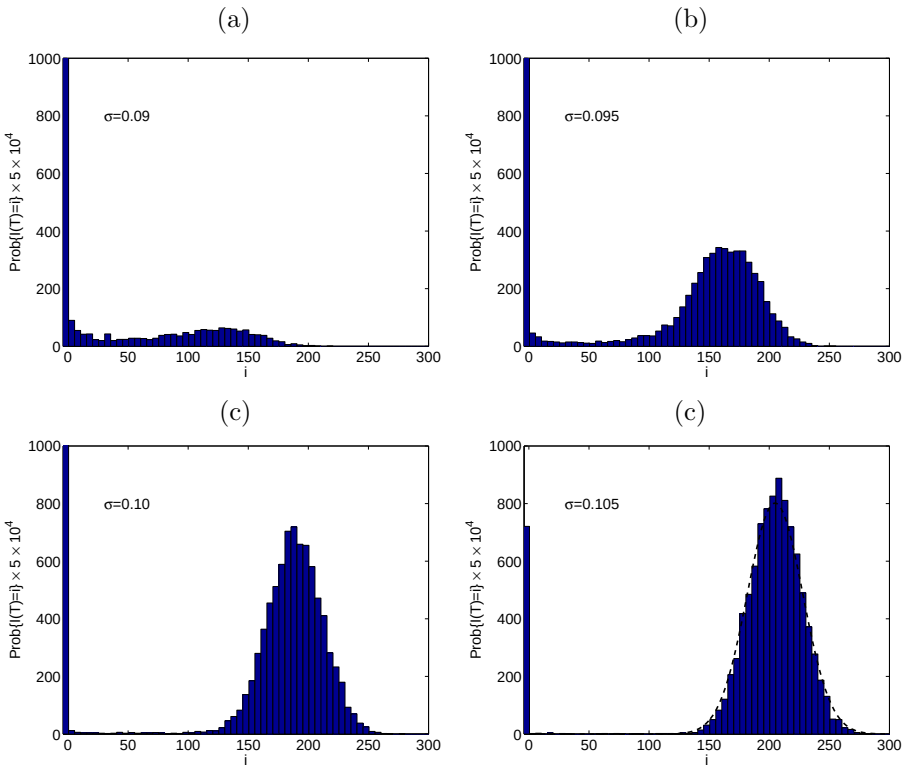

FIGURE 5. Probability distributions at five years for the number of infective individuals given $N = 1000$, Prob$\{\mathcal{I}(0) = 5\} = 1$, Prob$\{\mathcal{R}(0) = 0\} = 1$, and Prob$\{\mathcal{V}(0) = 500\} = 1$. (a) $\sigma = 0.09$, (b) $\sigma = 0.095$, (c) $\sigma = 0.10$. (d) $\sigma = 0.105$. The dashed curve in (d) is the normal approximation.

the population size, introduction of a small number of infective individuals into a population can have widely different longterm outcomes in the stochastic model, especially when the vaccine efficacy lies in the region of bistability.

Acknowledgments. This research was initiated by discussions at the Banff 2004 workshop on disease modeling. We thank Edward J. Allen, Texas Tech University, for assistance with the numerical simulations. LJSA acknowledges support from NSF grant DMS-0201105. PvdD acknowledges support from NSERC and MITACS.

REFERENCES

[1] J. Arino, C. C. McCluskey, and P. van den Driessche, GLOBAL RESULTS FOR AN EPIDEMIC MODEL WITH VACCINATION THAT EXHIBITS BACKWARD BIFURCATION. SIAM J Appl Math 64 (2003) 260-76.

[2] K. P. Hadeler and C. Castillo-Chavez, A CORE GROUP MODEL FOR DISEASE TRANSMISSION. Math Biosci 128 (1995) 41-55.

[3] K. P. Hadeler and P. van den Driessche, BACKWARD BIFURCATION IN EPIDEMIC CONTROL. Math Biosci 146 (1997) 15-35.

[4] E. J. Allen, Stochastic differential equations and persistence time for two interacting populations. Dyn Cont Discrete and Impulsive Systems 5 (1999) 271-81.
[5] N. Kirupaharan and L. J. S. Allen, Coexistence of multiple pathogen strains in stochastic epidemic models with density-dependent mortality. Bull Math Biol 66 (2004) 841-64.
[6] L. J. S. Allen, An Introduction to Stochastic Processes with Applications to Biology. Prentice Hall, Upper Saddle River, N. J., 2003.
[7] N. T. J. Bailey, The Mathematical Theory of Infectious Diseases and its Applications. Griffin, London, 1975.
[8] F. A. Ball, A note on the total size distribution of epidemic models. J Appl Prob 23 (1986) 832-36.
[9] D. J. Daley and J. Gani, Epidemic Modelling: An Introduction. Cambridge Studies in Mathematical Biology, Vol. 15. Cambridge Univ. Press, Cambridge, 1999.
[10] J. -P. Gabriel, C. Lefèvre, and P. Picard (Eds.), Stochastic Processes in Epidemic Theory. Lecture Notes in Biomathematics 86. Springer-Verlag, New York, Berlin, Heidelberg, 1990.
[11] J. Jacquez and C. P. Simon, The stochastic SI epidemic model with recruitment and deaths I. Comparison with the closed SIS model. Math Biosci 117 (1993) 77-125.
[12] C. J. Mode and C. K. Sleeman, Stochastic Processes in Epidemiology. HIV/AIDS, Other Infectious Diseases and Computers. World Scientific, Singapore, New Jersey, 2000.
[13] D. Mollison (Ed.), Epidemic Models: Their Structure and Relation to Data. Cambridge Univ. Press, Cambridge, 1995.
[14] I. Nasell, On the quasi-stationary distribution of the stochastic logistic epidemic. Math Biosci 156 (1999) 21-40.
[15] I. Nasell, A new look at critical community size for childhood infections. Theor Pop Biol 67 (2005) 203-16.
[16] M. E. Alexander, C. Bowman, S. M. Moghadas, R. Summers, A. B. Gumel, and B. M. Sahai, A vaccination model for transmission dynamics of influenza. SIAM J Appl. Dyn Sys 3 (2004) 503-24.
[17] V. Isham, Assessing the variability of stochastic epidemics. Math Biosci 107 (1991) 209-24.
[18] A. L. Lloyd, Estimating variability in models for recurrent epidemics: assessing the use of moment closure techniques. Theor Pop Biol 65 (2004) 49-65.
[19] J. M. Ortega, Matrix Theory a Second Course. Plenum Press, New York, 1987.
[20] T. C. Gard, Introduction to Stochastic Differential Equations. Marcel Dekker, Inc., New York and Basel, 1988.
[21] P. E. Kloeden and E. Platen, Numerical Solution of Stochastic Differential Equations. Springer-Verlag, New York, 1992.
[22] T. G. Kurtz, Limit theorems for sequences of jump Markov processes approximating ordinary differential processes. J Appl Prob 8 (1971) 344-56.
[23] S. M. Henson, A. A. King, R. F. Costantino, J. M. Cushing, B. Dennis, and R. A. Desharnais, Explaining and predicting patterns in stochastic population systems. Proc Roy Soc Lond B 270 (2003) 1549-53.
[24] S. M. Henson, J. R. Reilly, S. L. Robertson, M. C. Shu, E. W. D. Rozier, and J. M. Cushing, Predicting irregularities in population cycles. SIAM J Applied Dyn Sys 2 (2003) 238-53.

Received on March 31, 2006. Accepted on April 13, 2006.

E-mail address: linda.j.allen@ttu.edu
E-mail address: pvdd@math.uvic.ca